

Peak-Seeking Controller for Real-Time Mobile Satellite Tracking

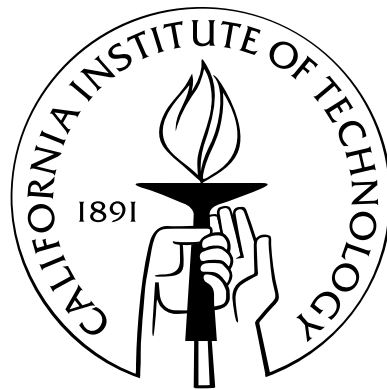
Thesis by

Robert F. Karol

In Partial Fulfillment of the Requirements

for the Degree of

Minor in Control and Dynamical Systems



California Institute of Technology

Pasadena, California

2012

(Submitted July 5, 2012)

© 2012

Robert F. Karol

All Rights Reserved

Acknowledgements

I would like to thank my mentor, Professor Richard Murray for his guidance and advise throughout the course of my Senior Thesis. I would also like to thank my Co-Mentor, Gunnar Ristroph for his support throughout the course of the research and for inspiring me to take on the conical scanning problem.

Abstract

Increasingly tightened restrictions on antenna beam-width force the use of higher performance hardware in gimballed satellite communication transceivers. The need for more precise hardware is forcing the price of gimbal-mounted satellites antennas higher. In addition to the increased cost, as more satellites are launched every year, the demand for antenna systems which can receive data from the new satellites grows. Although algorithms capable of tracking a satellite with a mobile antenna have been developed and characterized in detail, instabilities in the system and cross-axis effects degrade the performance. Since an increase in tracking capability would be most beneficial if it did not require extensive hardware changes, this project focuses on improvements to the conical scanning algorithm. An algorithm which is one of the oldest, and most common mobile satellite tracking system implementations. Initial work was done on developing and characterizing a new estimator which could be used while continuing to scan the antenna with as few software modifications as possible. After successful development, work was done to eliminate the induced scanning motion and gain observability in the system using nothing but the noise inherent in the system.

Contents

Acknowledgements	iii
Abstract	iv
1 Introduction	6
1.1 Problem	6
1.2 Background	7
1.3 Motivation	7
1.4 Literature Review	8
1.4.1 Conical Scanning	8
1.4.2 Parameter Estimation using Assumed Functions	9
1.4.3 Extended Kalman Filter	10
2 Problem Setup	11
2.1 Theoretical Setup	11
2.2 Variable Parameters	12
2.3 Analysis Methodology	12
2.4 Simulink Conventions	13
2.5 Stabilized Dynamics Block with Noise	13
2.5.1 Dynamics	13
2.5.2 Stabilizing Controller	14
2.5.3 Noise	14
3 Initial Simulations	16
3.1 Traditional Conical Scanning	16
3.1.1 Simulink Model	16
3.1.2 Advantages	16
3.1.3 Disadvantages	17
3.2 Predicted Gradient Conical Scanning	17
3.2.1 Simulink Model	18

3.2.2	Advantages	18
3.2.3	Disadvantages	19
3.3	Measured Gradient Conical Scanning	19
3.3.1	Simulink Model	19
3.3.2	Advantages	20
3.3.3	Disadvantages	20
3.4	Measured Gradient Tracking	20
3.4.1	Simulink Model	20
3.4.2	Advantages	21
3.4.3	Disadvantages	21
3.5	Preliminary Results	21
3.6	Overview of Approach	22
3.7	Performance Metrics	22
3.8	Top Level Block Diagram	23
3.9	System Dynamics Equations	23
4	Detailed Analysis of Traditional Conical Scanning	25
4.1	Estimator	25
4.2	Step Response	26
4.3	Ramp Response	29
4.4	Noise Response	30
4.5	Problems	30
5	Detailed Analysis of Gradient Conical Scanning	31
5.1	Estimator	31
5.2	Step Response	32
5.3	Ramp Response	34
5.4	Noise Response	35
5.5	Problems	36
6	Closed Loop Simulation	37

7	Conclusions and Future Direction	39
7.1	Conclusions	39
7.2	Future Work	40
7.2.1	Signal Saturation	40
7.2.2	Parameter Optimization	40
7.2.3	Measured Gradient Scanning and Tracking Systems	40
7.2.4	Hardware Implementation	41
	Bibliography	42

List of Figures

2.1	Theoretical problem setup.	12
2.2	Simulink model of the stabilized dynamics with noise.	14
3.1	Current implementation of the conical scanning system used for the JPL Deep Space Network. [3]	17
3.2	Simulink model of the predicted gradient conical scanning method.	18
3.3	Simulink model of the measured gradient conical scanning method.	19
3.4	Simulink model of the measured gradient tracking method.	21
3.5	Overall system design diagram for the conical scanning estimators to track to the origin.	23
4.1	The range measurement (signal strength) is convolved with the position perturbation.	25
4.2	Step response of the traditional conical scanning estimator with $\omega = 2\pi$ and $A = 0.1$ while varying ϕ	26
4.3	Step response of the traditional conical scanning estimator with $\omega = 2\pi$ and $\phi = \frac{3\pi}{2}$ while varying A	27
4.4	Cross-axis step response of the traditional conical scanning estimator with $\omega = 2\pi$ and $\phi = \frac{3\pi}{2}$ while varying A	28
4.5	Ramp response of the traditional conical scanning estimator with $\omega = 2\pi$ and $\phi = \frac{3\pi}{2}$ while varying A	29
4.6	Cross-axis ramp response of the traditional conical scanning estimator with $\omega = 2\pi$ and $\phi = \frac{3\pi}{2}$ while varying A	30
5.1	The range measurement (signal strength) is differentiated with respect to time before being convolved with the velocity perturbation.	31
5.2	Step response of the gradient conical scanning estimator with $\omega = 2\pi$ and $\phi = \frac{3\pi}{2}$ while varying A	33
5.3	Cross-axis step response of the gradient conical scanning estimator with $\omega = 2\pi$ and $\phi = \frac{3\pi}{2}$ while varying A	34

5.4	Ramp response of the gradient conical scanning estimator with $\omega = 2\pi$ and $\phi = \frac{3\pi}{2}$ while varying A	35
5.5	Cross-axis ramp response of the gradient conical scanning estimator with $\omega = 2\pi$ and $\phi = \frac{3\pi}{2}$ while varying A	35
6.1	Closed loop system of the traditional conical scanning estimator including tracking feedback.	37
6.2	Closed loop system of the gradient conical scanning estimator including tracking feedback.	37

1: Introduction

1.1 Problem

An antenna must be pointed in the direction of the signal's source in order to receive signals. The goal of mobile satellite communications systems is to keep an antenna pointed as closely as possible to a far target over an extended period of time. This target could be a boat, plane, satellite, or any other device which is broadcasting a signal. By inertially stabilizing the antenna with gyroscope feedback, the antenna can be kept pointing at its target over short time-scales. Over long time-scales, however, external disturbances begin to compound the drift and a long term tracking method must be used to keep the antenna pointing on target. Long term tracking is achieved through the use of an active control system which nutates the beam and estimates how well the antenna is aligned with the target by watching the resulting change in signal strength.

This work aims to develop a long term tracking algorithm from a theoretical framework. The framework chosen sets the problem up as a peak-seeking problem, where the goal is to minimize the distance to the satellite over all time. Similar peak seeking control problems used in other fields are discussed. One commonly implemented technique used in the radio frequency (RF) communications field, conical scanning, is analyzed in detail [3]. This detailed analysis provides performance characteristics which can be compared to new developments, and helps to reveal the problems with the original estimator that need to be resolved.

An improved algorithm is suggested and analyzed to show the response of the new estimator to the same situations that the traditional method was subject to. Increased performance parameters indicate the suitability of the new estimator, and the effects that these changes have on the closed-loop tracking system are discussed. This thesis does not attempt to find an optimal estimator, or a way of keeping an antenna pointed to its target that has better performance than any previously developed algorithms. Rather than finding a complex system that is difficult to implement, this work proposes a simple new solution. The new system has the potential for wide spread implementation on

current systems without the need for extensive hardware changes.

1.2 Background

Since the development of radar, methods for tracking vehicles have been needed for everything from communication systems to defense systems. Estimates of an object's location could be to pinpoint an enemy ship or relay messages to aircraft. The earliest radar needed to be pointed at the target by an operator. Thus, the operator had to know the location of the target. While this worked well for stationary dishes with fixed targets, this became difficult for longer range communication antennas and therefore a more sophisticated method for tracking became a necessity.

Conical scanning has become the most widely implemented method for satellite tracking due to its simplicity [3]. With nothing but a perturbing motion defined by two sine waves, which can be easily superimposed upon the tracking signals, a relatively stable controller can be implemented. This estimator has been used on everything from small mobile antennas mounted on military vehicles to the large 64-m diameter antennas used by NASA/JPL to communicate with spacecraft [3].

1.3 Motivation

For many Geosynchronous satellites and fixed antennas the dish can be manually pointed and locked into place but, when either the source or receiver is in motion, a tracking system is needed to keep the antenna on target. When mis-pointed, the strength of the received signal drops, reducing performance. Even when the path of a satellite is known, without feedback, the accumulation of error in location due to wind or other disturbances causes the antenna to drift off course and lose the signal. In order to prevent this the transmitting and receiving stations can broadcast their locations between each other continuously. However, this adds to the complexity of the system. It also reveals the location of the ground station to nearby observers which is undesirable for military applications.

Methods for tracking using only the Received Signal Strength (RSS) were developed

in order to avoid these problems [3]. The most commonly used RSS tracking method is known as conical scanning, which rotates the antenna around the current best estimate of the satellite’s location known as the boresight axis. By inducing this circling motion, the RSS changes with distance from the target. By convolving the RSS with the position offset wave in the x and y directions over a full cycle, it is possible to extract the phase offset, which can be used to estimate the location along each axis.

1.4 Literature Review

A number of different approaches to develop peak-seeking controllers have been developed for a variety of wide-spread applications ranging from communications links to dynamic optimization and formation flying techniques. Finding the location where a cost function is minimized or performance function is maximized is the goal of many systems. There are significant variations in methodology based on the specific problem being addressed. A method used for peak-seeking in a different field might apply to implementation on a mobile communications system.

The general problem of finding and staying at a peak is called “peak-seeking” in control literature, although this term is not used much in the gimbal pointing or tracking industry. An example of a similar problem comes from formation flight control[1]. Two aircraft seek to maximize the aerodynamic efficiency (reduce drag) by flying close to one another. The aerodynamic efficiency is maximized at a particular relative position, which cannot be known exactly *a priori* and may move slowly with changing parameters.

1.4.1 Conical Scanning

Conical scanning is one of the most commonly implemented systems, and the one which was analyzed most thoroughly during the course of this research. This method works by comparing the motion of the scan to the change in received signal along the elevation and cross-elevation axis. If the signal strength drops as the antenna is moving to the left, the satellite must be located to the right of where it is pointed. Alternatively, if the signal strength increases, then the satellite position is farther left. By averaging the left-right estimate over a full scan, an estimate of the location of the satellite with respect

to the scanning axis is generated. This process of keeping the signal “peaked up” is called tracking and consists of convolving the received signals with the antenna’s perturbations. [2].

One of the most thorough analyses of conical scanning was done as a technical report released by NASA/JPL in 1976 [3]. This report documents the work which was done to demonstrate the feasibility of using conical scanning on the 64-meter diameter paraboloid antenna at Goldstone, California. The report describes how the system was perturbed, and the effect which the scanning rate, as well as the scanning radius had on performance without assuming a shape for the signal strength. A detailed analysis of the noise performance was carried out along with a comparison to experimental results.

Although the application was for fixed Earth stations (not mobile, with no stabilization), the tracking algorithm is the same as is used on many mobile antennas. NASA/JPL have since researched and implemented a variety of other tracking techniques. Rather than using a naïve correlation, these more advanced architectures use a Kalman filter formulation for the estimator.

1.4.2 Parameter Estimation using Assumed Functions

Chichka et al. at the University of California, Los Angeles investigated formation flying techniques in 2006. Rather than attempting to model the system perfectly, they constructed functions of the form which they expected, but without choosing values for the individual parameters [1]. By calculating these parameters online, they were able to adapt as unknown factors began arising. A method for using an adaptive loop that calculates the parameters and how they change over time was provided.

This technique became problematic during implementation. In particular it was designed to allow the parameters to vary over time, which while it helped optimize the system when atmospheric attenuation problems arose, also obscured the definitive robustness and stability parameters. Additionally, the nature of the antenna communication problems eliminated the need for online calculations of the initial function since the shape could be determined through simple system identification techniques.

1.4.3 Extended Kalman Filter

One method for estimating the position is to use an extended Kalman filter to keep track of the best location estimate as well as the error from various sources. An analysis of this method was carried out for use in pointing a laser beam at an optical position sensor which underwent dynamic disturbances. Light intensity was used as feedback [4]. This method is similar to the proposed mobile communications infrastructure where the signal is strongest with perfect pointing, and drops off as the laser gets farther from the target.

The method proposed in the paper, “Laser Beam Pointing and Stabilization by Intensity Feedback Control,” [4] discusses the advantages and disadvantages of using an extended Kalman filter observer for pointing the laser. The biggest drawback to this approach was that it was not possible to steer the laser to the optimal operation point due to the symmetry inherent in the situation. However, they were able to steer to sub-optimal operation points which helped to bound the total amount of accumulating error so it improved upon an open loop system.

While the setup was designed for a mobile communications framework, the implementation of this method was more complex than the more standard conical scanning methods, and did not provide any particular advantage over the conical scanning method. Rather than analyzing this method in detail, it may be more beneficial to incorporate extended Kalman Filter observers on top of a new method.

2: Problem Setup

2.1 Theoretical Setup

I took a theoretical approach to solving this problem, starting with the fundamental method of trying to estimate an (x, y) position, with nothing but a measurement of distance from the origin. This measurement was obtained from the signal strength. The velocities in each direction were taken from gyroscopes. Figure 2.1 shows the theoretical problem setup. For a real system, the following sensors and actuators would be present which could be transformed onto a Cartesian coordinate system with the following values. For now, it is assumed that the Received Signal Strength can be modeled as r^2 and the controller is trying to minimize

$$\int_{t_0}^{t_f} r^2 dt. \quad (2.1)$$

- **Gyroscope Sensors:** \dot{x}, \dot{y}
- **Received Signal Strength:** $x^2 + y^2$
- **Actuators:** T_x, T_y
- **Disturbances:** D_x, D_y
- **Process Dynamics:** $\ddot{x} = T_x + D_x, \ddot{y} = T_y + D_y$

The following methods explore the advantages and disadvantages of conical scanning, as well as new proposed alternative methods for RSS tracking. These methods were developed to eliminate some of the problems which arise using the traditional conical scanning methods.

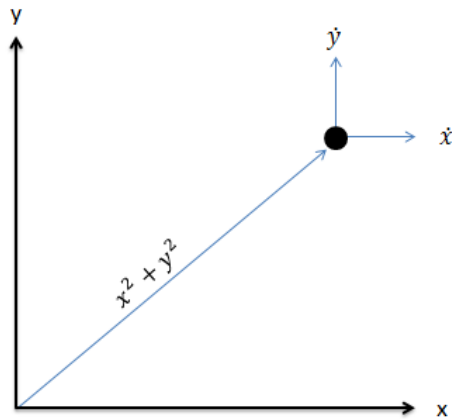


Figure 2.1: Theoretical problem setup.

2.2 Variable Parameters

In order to characterize each of these methods, it is important to keep in mind which parameters can be changed to optimize a given system. While the simulations give a baseline set of characteristics to compare, each antenna will have different properties, and depending on the intended application, a single method may not be optimal in all cases. By considering the advantages and disadvantages of each estimator, the gains and method can be chosen for the task.

- A : The amplitude of the perturbation and convolved waves.
- ω : The scanning frequency in radians / second.
- X_0, Y_0 : The position which the scanning takes place around. This information is not available to the estimator, but is used for simulating the path.

2.3 Analysis Methodology

In each of the following sections a different estimator was analyzed to identify its advantages and disadvantages. For each of the proposed methods a Simulink model was used to analyze the tracking ability of the system using different estimator gains. The Simulink model is provided as well as a list of advantages and disadvantages for each method.

Most of these approaches follow the basic block diagram shown in figure 3.8. These approaches implicitly or explicitly produce some estimate of position x and y .

2.4 Simulink Conventions

While many of the Simulink blocks are standard the following blocks have the listed parameters.

- **x pos wave:** $A \cos(\omega t) + X_0$
- **y pos wave:** $A \sin(\omega t) + Y_0$
- **x vel wave:** $-A\omega \sin(\omega t)$
- **y vel wave:** $A\omega \cos(\omega t)$
- **Delay:** The delay block inserts a time delay into the system in order to integrate over the proper time range t_0, t_f .
- **Band-Limited White Noise:** Simulates Band-Limited White Noise with a power spectral density as listed to get the desired noise characteristics.

2.5 Stabilized Dynamics Block with Noise

While the estimator and tracking characteristics change for each simulation, the internal dynamics and noise inherent to the system have been kept consistent. Figure 2.2 is the Simulink model which shows the dynamics of the system, implements a stabilizing controller, and contains three types of noise with varying properties.

2.5.1 Dynamics

The dynamics of the system are given by integrators, which take the current forces applied by the torque from the motor and give out the sensor measurements measured by the gyroscopes, as well as a second integrator which keeps track of the (x,y) position throughout the simulation in order to extract the measurement of received signal strength.

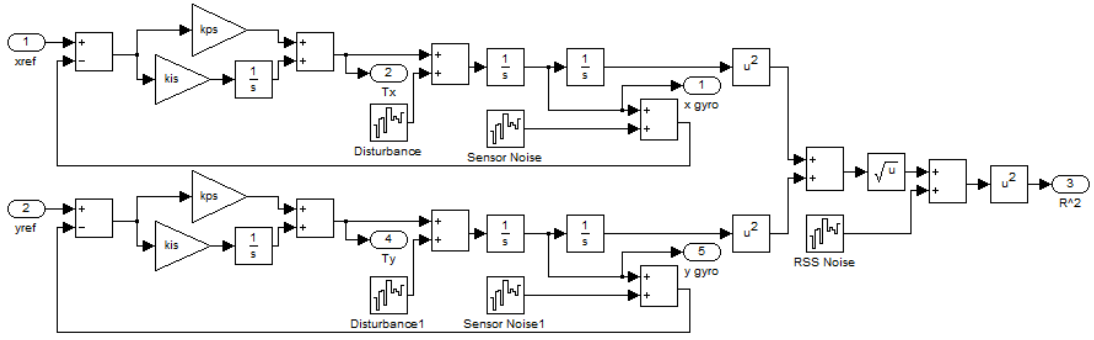


Figure 2.2: Simulink model of the stabilized dynamics with noise.

2.5.2 Stabilizing Controller

A PI controller was designed to give the system 20 Hz of bandwidth with a 60° phase margin in order to stabilize the system. The following choice of parameters results in a system with the desired characteristics.

$$K_P + \frac{K_I}{s} \quad (2.2)$$

. where $K_P = 86.6$, $K_I = 5000$.

2.5.3 Noise

Three different types of noise were included within this simulation. They were chosen in order to simulate the effects of various factors on a real system.

- **Sensor Noise:** The sensor noise was modeled to simulate the noise in the output signals from the gyroscopes. The power spectral density of this noise was chosen so the random drift in the position incurred by the noise was approximately 1 milli-radian of drift over 2 seconds.
- **Disturbances:** The disturbance noise arises from external torques applied to the antenna causing it to accelerate. In a real system, this noise could be a result of the wind. This noise was modeled so that there would be about 10 micro-radians of drift over 2 seconds.

- **Noise in the received signal:** The model of the received signal was disturbed by atmospheric effects over time. We introduced the RSS noise in order to have a RMS error of 40 micro-radians in the estimated radius.

3: Initial Simulations

3.1 Traditional Conical Scanning

A simulation of the traditional method of conical scanning was used on the JPL Deep Space Network [3]. As can be seen in figure 3.1, the reference velocity was chosen to be the derivative of the position offset. The desired position signal was then convolved with the RSS signal to get an estimate of position.

Along the x-axis, the offset wave is $A \cos(\omega t)$, which is positive for the first half cycle and negative for the second. Conical scanning compares the relative magnitude of the RSS when the antenna is pointed right of the boresight axis to when the antenna is pointed left. Along the y-axis, the offset wave is $A \sin(\omega t)$, which is positive when the antenna is pointed above the boresight axis and negative when it is pointed below.

3.1.1 Simulink Model

The Simulink model, which demonstrate the perturbations and traditional conical scanning estimator, is shown in figure 3.1. The velocity perturbations are fed through the process block before being estimated by convolving the received signal with the position perturbation and multiplying it by a gain. This model has unity feedback for simulation purposes, however, better tracking performance could be achieved by adding a feedback term.

3.1.2 Advantages

This method will be considered the baseline to which the new alternatives will be compared. Conical scanning has good tracking characteristics as well as disturbance rejection in the RSS signal which allows it to work even with imperfect conditions such as atmospheric disturbances. Faster conical scanning rates, and larger deviations from the boresight axis allow for faster tracking, and position updates can be made.

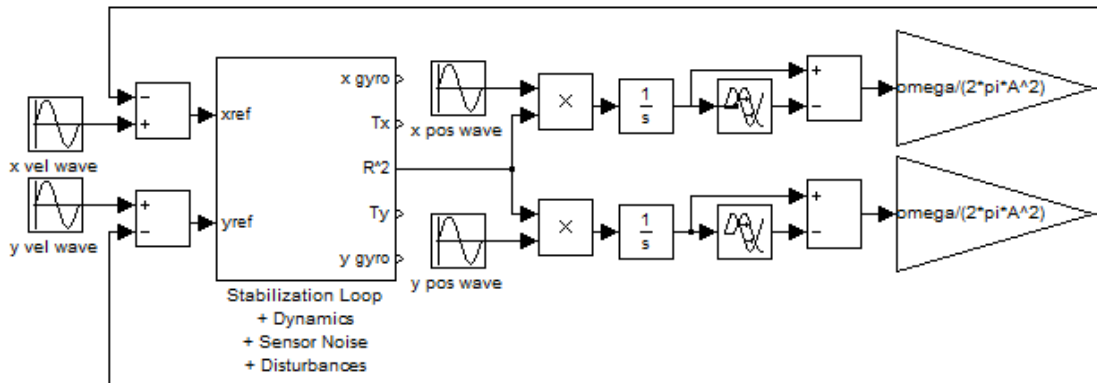


Figure 3.1: Current implementation of the conical scanning system used for the JPL Deep Space Network. [3]

3.1.3 Disadvantages

The largest disadvantage with conical scanning is the increase in error for real time sensing because the extra position offset is added to the inherent noise in the system. Even if the position estimate for the satellite is perfect, the constant scanning means the antenna will always be off center by a constant distance. When the target and receiver are stationary, scanning can be periodic, and the antenna can be directed back to the boresight axis after finding the highest signal strength if the disturbances accumulate slowly.

In addition to artificially adding an error term, the tracker does not provide an estimate which is proportional in each dimension. This causes the motion in one of the two axes to be significantly faster than the other, which becomes apparent in the simulation as a curved path to the peak in signal strength. This indirect path causes the antenna to accumulate error more quickly and lose tracking ability for a moving receiver.

3.2 Predicted Gradient Conical Scanning

In an attempt to eliminate some of the disadvantages associated with traditional conical scanning, a different set of signals were convolved. Rather than convolving the position offset wave with the RSS, the velocity wave used to produce the position offset was convolved with the derivative of the RSS. A model showing how this is implemented is shown in figure 3.2.

3.2.1 Simulink Model

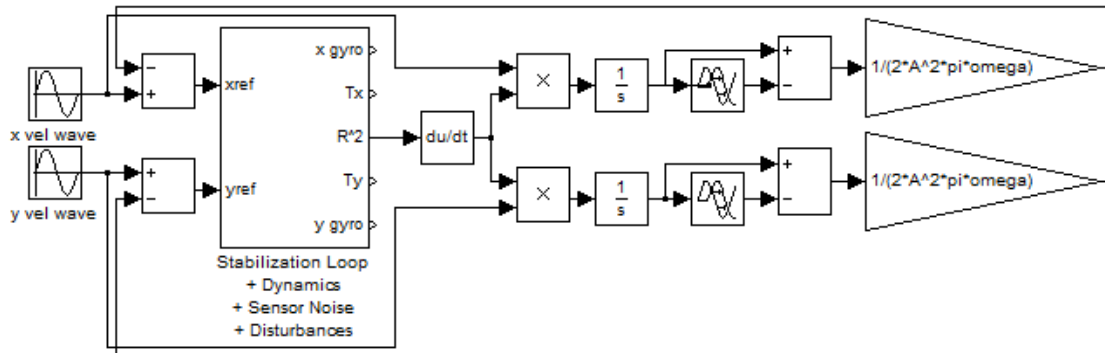


Figure 3.2: Simulink model of the predicted gradient conical scanning method.

3.2.2 Advantages

The simulation of this method revealed similarities to the closed loop traditional conical scanning simulation shown in figure 3.1. The noticeable advantages attained by changing the estimator showed up in the tracking capabilities. While movement to the origin was similar in magnitude, higher gains could be added to the feedback before the system became unstable. This advantage seemed to be due to the fact that by taking the derivative of the received signal, the magnitude of the convolved signal was significantly reduced. By reducing the tracking signal, a larger feedback gain would reproduce similar tracking characteristics.

The two most important apparent advantages came from the path that the tracker followed. Instead of following a curved path to the origin, the estimator seemed to go more consistently straight towards the origin in a way such that the velocity of the tracker in each direction was directly proportional to its offset in that direction. This motion helped to keep the system stable under increased feedback gains, and reduced the accumulation of error.

A second advantage of the alternative estimator is that the amplitude of the perturbations seem to have less effect on the tracking capabilities. Reducing the amplitude does not seem to reduce the stability of the system even when noise is added.

3.2.3 Disadvantages

The disadvantage associated with this method, which was not present in the traditional conical scanning method, arose from taking the derivative of the RSS signal. If the received signal is particularly noisy, taking the derivative could introduce even more noise. This extra noise could cause the system to go unstable unless steps were taken to reduce this effect. One possible solution could be to limit the output signal.

3.3 Measured Gradient Conical Scanning

One of the biggest advantages of convolving the velocity wave with the derivative of the RSS is that the gyroscopes in the system provide a direct measurement of the velocity. Rather than using the reference velocity, the measured velocity given by the gyroscopes can be used. This is something that can not be used in the traditional conical scanning methodology since the position perturbation is convolved.

3.3.1 Simulink Model

Figure 3.3 shows how the output from the gyroscope can be redirected and used in the estimator. This should have very little effect when done without noise as the gyroscope should perfectly reflect the predicted motion. However, when noise is added it propagates through the system dynamics and appears in the gyroscope signal.

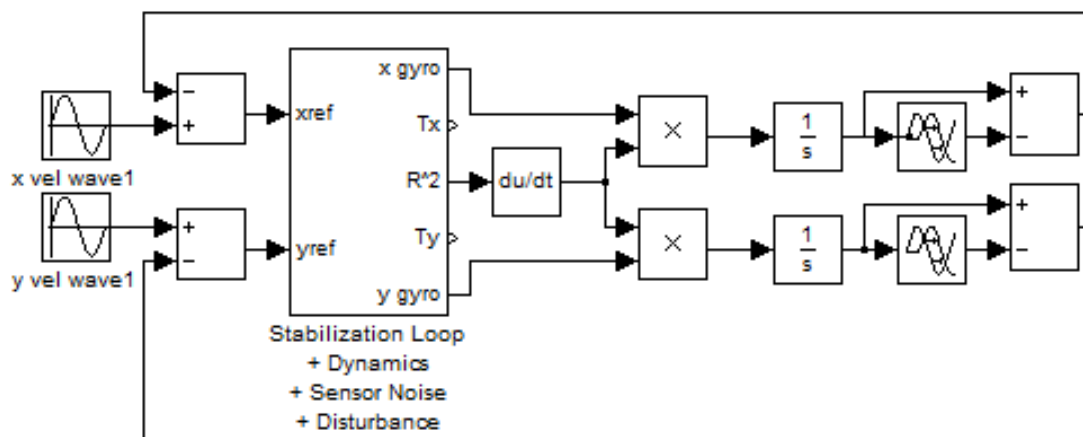


Figure 3.3: Simulink model of the measured gradient conical scanning method.

3.3.2 Advantages

By convolving the measured velocities in both direction, some of the symmetry in the previous problems is broken, allowing for the estimator to track along a much more direct path. Rather than curving off to the side, the antenna follows a direct path along the gradient of the RSS, which for circularly symmetric signals sends it to the peak at the origin.

The other advantage attained by using the measurements apparent through simulation is that noise in the system arises in both of the convolved signals, and as such seems to have less effect on the tracking ability than in the traditional conical scanning. This is similar to the predicted gradient conical scanning method. The noise seems to add observability to the system rather than destabilize the system.

3.3.3 Disadvantages

The biggest drawback to this method is that taking the derivative of the RSS signal which as in the predicated gradient conical scanning case can create very noisy signals.

3.4 Measured Gradient Tracking

In this method, when feeding the measured velocities into the convolution, the inherent noise in the system is used in observing position. In this case rather than rotating the antenna about a bore axis, white noise is used to simulate effects of noise in the system, and to help the system start tracking.

3.4.1 Simulink Model

The Simulink model shown in figure 3.4 eliminates the perturbing circulation term, but keeps the rest of the simulation the same. When no noise is present in the system, nothing changes as the lack of motion removes all observability, however, the noise internal to the process block adds an initial perpetuation. This noise adds enough observability that the antenna is able to estimate its position and track to the origin.

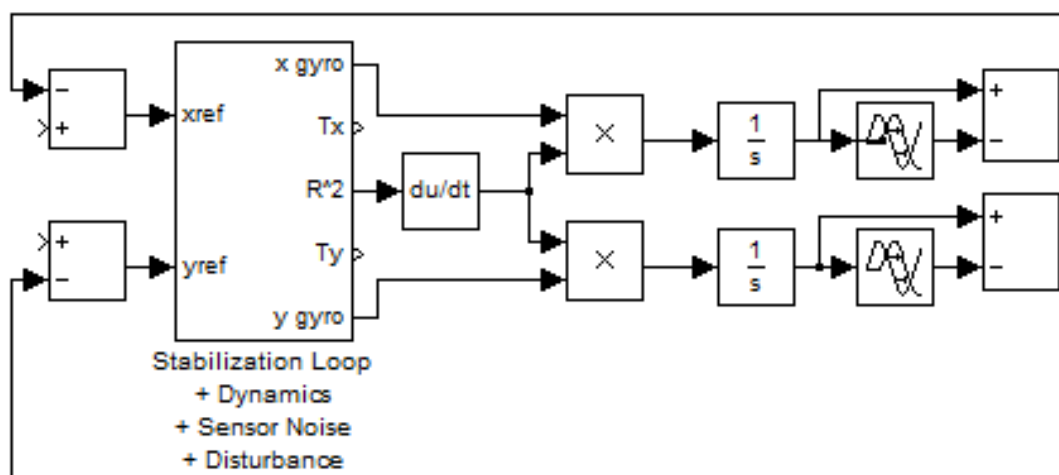


Figure 3.4: Simulink model of the measured gradient tracking method.

3.4.2 Advantages

By using band-limited white noise as the reference velocity, the need for introducing an extra error term is eliminated if the noise models the natural noise inherent in the system. If the internal noise is not high enough to provide observability, an additional white noise term can be added as the reference velocity connecting to the input port on the left of figure 3.4. This method still seems to provide an advantage over the measured gradient conical scanning method as a white noise input will keep the antenna pointed closer to on target on average than a forced circulation.

3.4.3 Disadvantages

The same drawback that the other gradient methods had of taking derivative of noisy signals is enhanced in this case. In addition to a noisy RSS feed, a noisy velocity measurement arises from the reference velocity, and the system loses some the predictability in its tracking performance.

3.5 Preliminary Results

The initial simulations of each method presented evidence that the new estimators improved upon the traditional conical scanning estimator. At a minimum, each estimator

seems to have its own set of advantages which could be utilized based on the desired pointing requirements. Based on the preliminary results, a more detailed mathematical analysis was performed and is provided as follows in order to compare the traditional conical scanning estimator to the newly proposed gradient conical scanning estimator.

3.6 Overview of Approach

Both solutions have inner stabilization loops for \dot{x} and \dot{y} which will be left out for the purpose of this analysis since the simulation is performed with no noise, effectively removing the effects of the inner stabilization loop. Both solutions use a circular scan in x and y to gain observability. By keeping as many parameters constant as possible the following performance metrics will be determined.

3.7 Performance Metrics

- Steady State Response: Estimate produced after a full cycle while the system is in steady state conditions should match the real position exactly.
- Step Response: The step response in x from a unit input in the satellites position along x should remain near the range of $[0, 1]$.
- Ramp Response: The ramp response of the x estimator due to motion along the x axis should stay bounded around the position of the satellite over time.
- Cross-Axis Step Response: The step response in x from a unit input in the satellites position along y should remain near the range of $[0, 1]$.
- Cross-Axis Ramp Response: The ramp response of the x estimator due to motion along the y axis should stay bounded around the position of the satellite over time.
- Noise Response: The estimator should reject enough noise which is propagating through the system as possible so the noise does not cause the system to go unstable.

3.8 Top Level Block Diagram

Both axes have an inner, fast stabilization loop. The outer tracking loop compensation acts to keep the system at $x = 0, y = 0$ by commanding the stabilization (velocity) loop. The perturbation generation commands the inner loop as well and creates the dithering or scanning motion. The Estimator observes the scanning action and $x^2 + y^2$ to estimate position for the outer loop to use as can be seen in figure 3.8

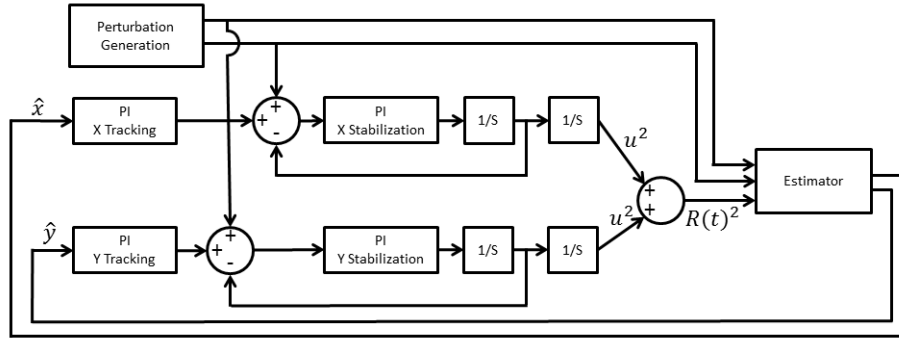


Figure 3.5: Overall system design diagram for the conical scanning estimators to track to the origin.

3.9 System Dynamics Equations

Equations 3.1 and 3.2 show the position perturbation around the boresight axis induced by moving the antenna with sinusoidal signals in both the x and y axis. The circular scanning motion is characterized by two parameters: the frequency (ω) and amplitude (A). The frequency clearly should not be beyond the stabilization loop bandwidth because then the stabilization loop would not be able to keep up with the commanded perturbation motion. Increasing the amplitude increases the effective signal to noise ratio, but is undesirable because it means that the antenna spends more time away from the ideal position. The equations that are used to model the perturbations are given by

$$x_{perturb}(t) = A \cos(\omega t + \phi) \quad (3.1)$$

and

$$y_{\text{perturb}}(t) = A \sin(\omega t + \phi). \quad (3.2)$$

In the steady-state with no noise, by adding these perturbations to our initial position (x_0, y_0) we get equations 3.3 and 3.4 showing the location the antenna is pointing over all time for $x(t)$

$$x(t) = x_0 + x_{\text{perturb}}(t) = x_0 + A \cos(\omega t + \phi) \quad (3.3)$$

and $y(t)$

$$y(t) = y_0 + y_{\text{perturb}}(t) = y_0 + A \sin(\omega t + \phi). \quad (3.4)$$

Combining these two equations gives

$$R(t)^2 = x(t)^2 + y(t)^2 = (x_0 + A \cos(\omega t + \phi))^2 + (y_0 + A \sin(\omega t + \phi))^2. \quad (3.5)$$

4: Detailed Analysis of Traditional Conical Scanning

4.1 Estimator

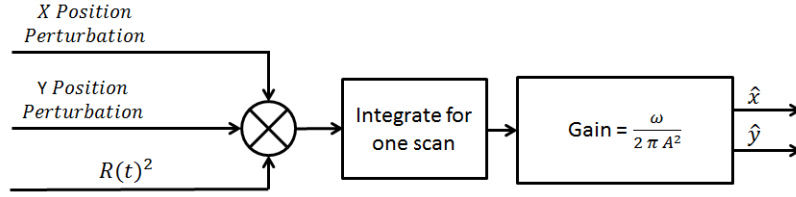


Figure 4.1: The range measurement (signal strength) is convolved with the position perturbation.

Under the traditional method of conical scanning, the signal strength R^2 is convolved with the position perturbation ($x_{perturb}$, $y_{perturb}$) and integrated over a full scan in order to get a position estimate (\hat{x} , \hat{y}). Figure 4.1 shows an overview of the estimator which takes in the received signal and convolves it with the position perturbation signals in order to get an estimate of the current position.

Equations 4.1 and 4.2 show the most general form for the estimator of both \hat{x}

$$\hat{x}(t) = \frac{\omega}{2\pi A^2} \int_{t-\frac{2\pi}{\omega}}^t R(\tau)^2 x_{perturb}(\tau) d\tau \quad (4.1)$$

and \hat{y}

$$\hat{y}(t) = \frac{\omega}{2\pi A^2} \int_{t-\frac{2\pi}{\omega}}^t R(\tau)^2 y_{perturb}(\tau) d\tau. \quad (4.2)$$

Maintaining the assumption that the system is at steady state without noise, it becomes possible to substitute in equations 3.5, 3.1, and 3.2 to get equations 4.3, and 4.4. These equations show that with the gain factor of $\frac{\omega}{2\pi A^2}$ was chosen so that $\hat{x} = x_0$ and $\hat{y} = y_0$ after a single cycle are given by

$$\hat{x}(t) = \frac{\omega}{2\pi A^2} \int_{t-\frac{2\pi}{\omega}}^t ((A \cos(\omega\tau + \phi) + x_0)^2 + (A \sin(\omega\tau + \phi) + y_0)^2) A \cos(\omega\tau + \phi) d\tau = x_0 \quad (4.3)$$

and

$$\hat{y}(t) = \frac{\omega}{2\pi A^2} \int_{t-\frac{2\pi}{\omega}}^t ((A \cos(\omega\tau + \phi) + x_0)^2 + (A \sin(\omega\tau + \phi) + y_0)^2) A \sin(\omega\tau + \phi) d\tau = y_0. \quad (4.4)$$

4.2 Step Response

While the steady state response of the estimator is perfect, an actual system will be moving through a combination of controlled motion during tracking, and noise introduced into the system by external torques. In order to determine the effects of this motion it becomes important to analyze the transient response.

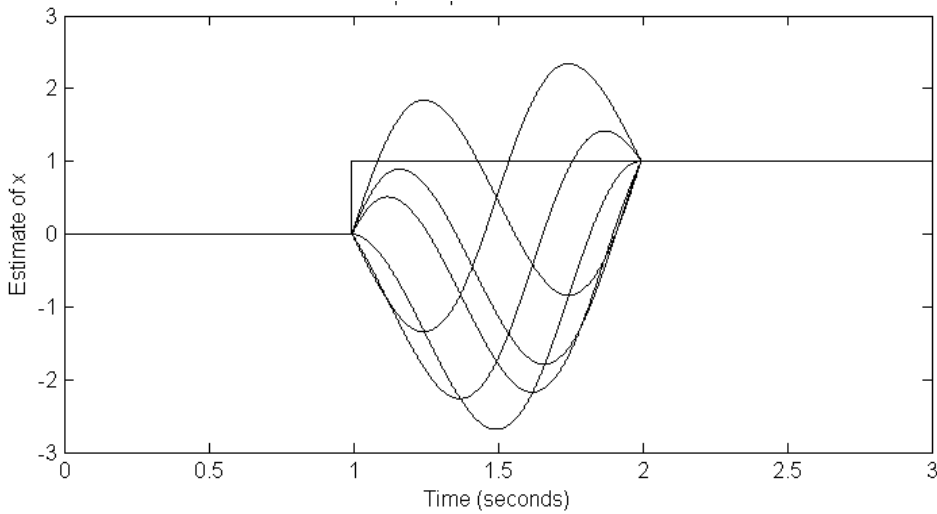


Figure 4.2: Step response of the traditional conical scanning estimator with $\omega = 2\pi$ and $A = 0.1$ while varying ϕ .

Figure 4.2 shows how the step response varies with ϕ . This indicates the position over the scan at which the step occurs since the step response when the y perturbation is maximum as compared to when the x perturbation is maximum. For all simulations performed on both the traditional conical scanning estimator, and the gradient conical

scanning estimator, varying ϕ had a similar affect. The curve shifted, but had similar characteristics for a fixed A and estimator.

For purposes of the analysis $\phi = \frac{3\pi}{2}$ was chosen as it depicts one of the worst case step and ramp responses for the traditional conical scanning estimator. This occurs because the step response continuously overestimates the actual position due to the convolution method. While the problems discussed in the following sections occur over a large range of values for ϕ , the differences are easiest to see with this particular value.

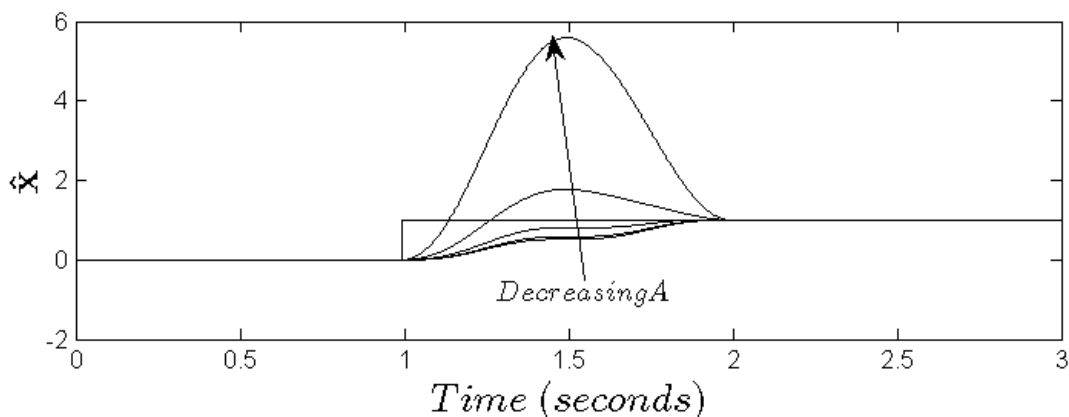


Figure 4.3: Step response of the traditional conical scanning estimator with $\omega = 2\pi$ and $\phi = \frac{3\pi}{2}$ while varying A .

Figure 4.3 shows the step response of the traditional conical scanning estimator when scanning with a few different radii. For all future plots with varying A , the following values will be used $A = (1/16, 1/4, 1, 4, 16)$. $A = 1$ is the same as setting the radius of the scan equals the size of the step taken.

Figure 4.3 shows some of the problems which arise using the traditional estimator. While the estimator works well for large values of A , as A is decreased, the transient response gets worse. When $A = 1/16$ of the step size, $\frac{\hat{x}}{x_{actual}} > 5$ this proves problematic as any tracking loop will have to be slow enough to smooth out these large variations, and robust enough that the system will not go unstable.

After looking at the step response of the system, it is important to look at the cross-axis step response. This shows the transient response in the estimate of y due to a step response in x . Figure 4.4 shows how the cross-axis step response varies for different values of A . While the cross-axis step response does not have the same problems of estimating a

position which is always too high or too low, it does grow unbounded for smaller A . This figure indicates that the estimates of x and y are coupled which could create instabilities in the system. It is this feature of the traditional estimator which causes the asymmetric tracking motion and generates a curved track to the origin increasing the amount of accumulated error.

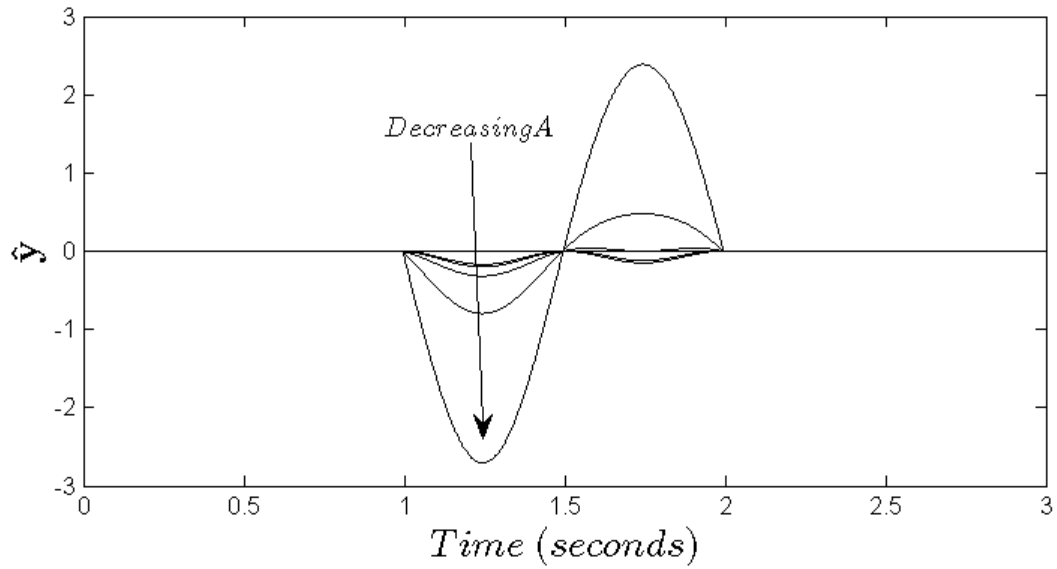


Figure 4.4: Cross-axis step response of the traditional conical scanning estimator with $\omega = 2\pi$ and $\phi = \frac{3\pi}{2}$ while varying A .

4.3 Ramp Response

The ramp response of the system is generated by providing an input of 1 radius / cycle to the origin. This shows how the system would respond if the target was moving, or when the tracking feedback is pushing the boresight axis toward the origin.

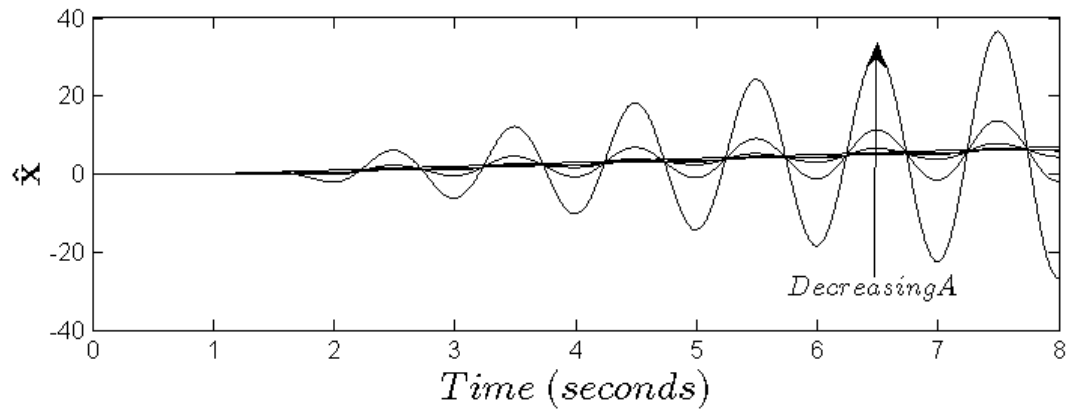


Figure 4.5: Ramp response of the traditional conical scanning estimator with $\omega = 2\pi$ and $\phi = \frac{3\pi}{2}$ while varying A .

When using the traditional estimator, figure 4.5 shows how the error compounds over time. This causes the estimate to grow unbounded over time, and decrease the viability of the estimate. Within just six cycles with a small value of A (simulating a fast moving tracker) the estimate is off by nearly an order of magnitude. This estimate would quickly become unusable as it would cause system instability if fed back to the tracker.

The accumulating error in the cross-axis response is unbounded and indicates the closed loop system would go unstable when the ratio of $\frac{A}{StepSize}$ is small. During tracking the system is constantly in motion, which makes the transient response for motion is quite important.

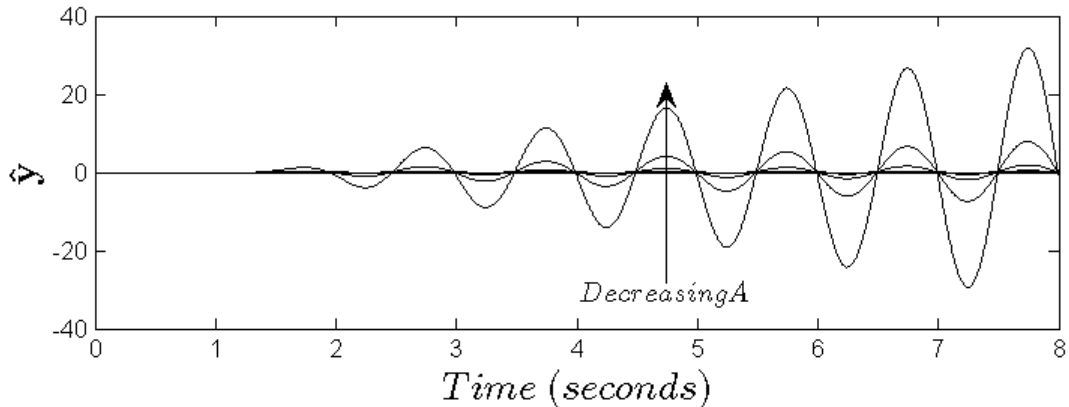


Figure 4.6: Cross-axis ramp response of the traditional conical scanning estimator with $\omega = 2\pi$ and $\phi = \frac{3\pi}{2}$ while varying A .

4.4 Noise Response

Through simulation it was apparent that whenever the radius of the perturbing term was reasonably large in comparison to the amount of noise in the system, most of the noise was smoothed out through the estimator. The noise used for this simulation was band-limited white noise of the type described in section 2.5. Since the estimator is able to smooth out some of the noise, and the closed loop system acts as a low pass filter, the simulation is fairly robust to noise introduced to the system.

4.5 Problems

The traditional estimator works very well under conditions where the radius of the scan is comparable to or larger than the motion caused by tracking or external noises, however, figure 4.3 shows how far off the estimator can be when the radius of the scan is too small. While this problem could be overcome by using a large scanning radius, larger scans prevent the antenna from pointing directly at the origin since during the scan. The antenna is constantly being forced away from the best estimate by the radius of the scan.

The asymmetry in the step response, and the ramp response results in curved trajectories increasing the total accumulated error. The error in the position estimate create instabilities like the ones in the transient responses when tracking too quickly. The discussion in chapter 6 goes into detail on how these instabilities limit the tracking feedback.

5: Detailed Analysis of Gradient Conical Scanning

5.1 Estimator

A new estimator was designed to help eliminate some of the problems that arose using the traditional method many of which are due to the fact that the R^2 term is unbounded and increases quickly while moving away from the origin.

Rather than using the value of the received signal strength $R^2(t)$ directly, the new conical scanning estimator uses the derivative of the received signal $\frac{d}{dt}[R(t)^2]$ strength, and convolves it with the velocity perturbation signal $(\frac{d}{dt}[x_{perturb}], \frac{d}{dt}[y_{perturb}])$ over one scan in order to estimate the current position. Figure 5.2 shows a schematic for the new estimator which has a different gain, as well as different signals to convolve.

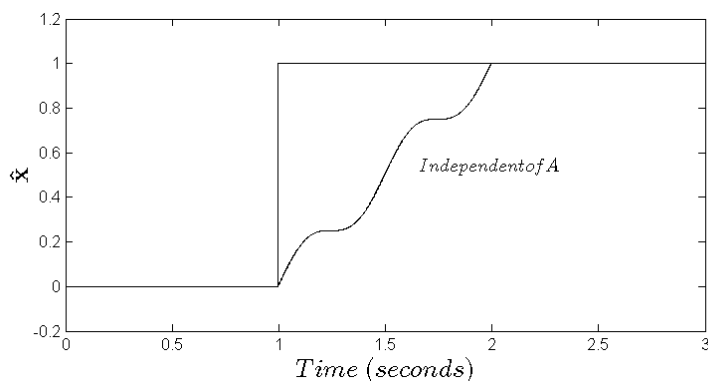


Figure 5.1: The range measurement (signal strength) is differentiated with respect to time before being convolved with the velocity perturbation.

The most general form of the gradient conical scanning estimator is given by equations 5.1 and 5.2 with the equations

$$\hat{x}(t) = \frac{1}{2\pi A^2 \omega} \int_{t-\frac{2\pi}{\omega}}^t \frac{d}{d\tau}[R(\tau)^2] \frac{d}{d\tau}[x_{perturb}(\tau)] d\tau \quad (5.1)$$

and

$$\hat{y}(t) = \frac{1}{2\pi A^2 \omega} \int_{t-\frac{2\pi}{\omega}}^t \frac{d}{d\tau} [R(\tau)^2] \frac{d}{d\tau} [y_{\text{perturb}}(\tau)] d\tau. \quad (5.2)$$

As with the traditional conical scanning estimator, by making the assumption that the system is at steady state with no noise, we can substitute equations 3.5, 3.1, and 3.2 into the estimator. After substituting in equations 3.5, 3.1, and 3.2 we get equations 5.3 and 5.4. These equations

$$\hat{x}(t) = \frac{1}{2\pi A^2 \omega} \int_{t-\frac{2\pi}{\omega}}^t \frac{d}{d\tau} [(A \cos(\omega\tau) + x_0)^2 + (A \sin(\omega\tau) + y_0)^2] (-A\omega \sin(\omega\tau)) d\tau = x_0 \quad (5.3)$$

and

$$\hat{y}(t) = \frac{1}{2\pi A^2 \omega} \int_{t-\frac{2\pi}{\omega}}^t \frac{d}{d\tau} [(A \cos(\omega\tau) + x_0)^2 + (A \sin(\omega\tau) + y_0)^2] (A\omega \cos(\omega\tau)) d\tau = y_0 \quad (5.4)$$

show that this estimator is also able to perfectly estimate position after a single cycle. Therefore, the estimator is able to perfectly predict position while it is at steady state with no noise.

5.2 Step Response

The step response for the new estimator can be seen in figure 5.2 with the same properties used in figure 4.3.

The step response shown in figure 5.2 has a significant improvement over the step response of the traditional conical scanning estimator in figure 4.3. Rather than performing worse when smaller values of A are used, the step response is independent of A . This would indicate that rather than becoming unstable if more noise were to very quickly move the antenna beyond the scanning radius, the estimator would work just as well as if the step response induced by the noise was much smaller. This is an important characteristic of the estimator as it is able to estimate the step response well regardless of the size of the jump. Additionally, since the step response is independent of A a smaller conical scanning radius can be used which keeps the antenna pointed closer to the estimated position and improves the overall received signal strength.

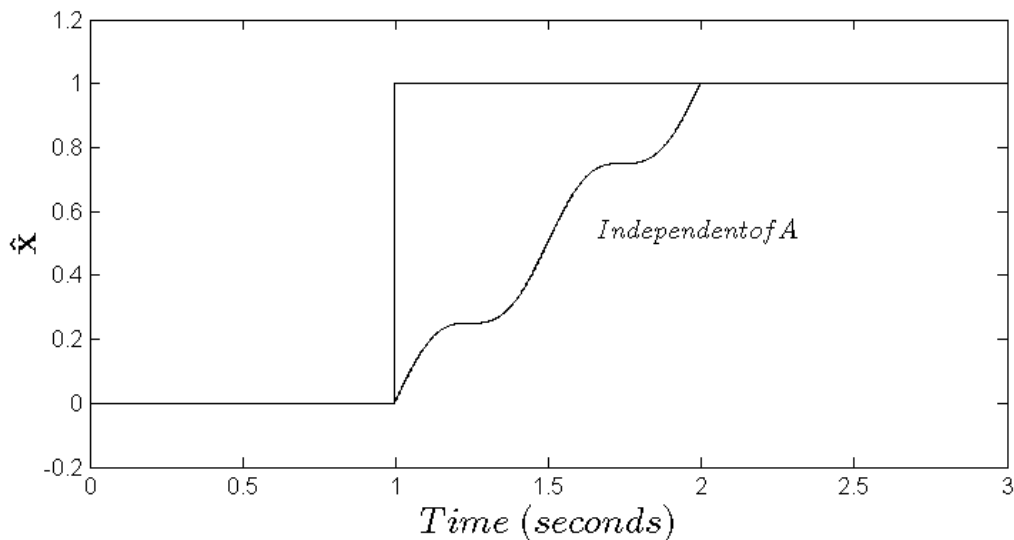


Figure 5.2: Step response of the gradient conical scanning estimator with $\omega = 2\pi$ and $\phi = \frac{3\pi}{2}$ while varying A .

While the step response has good characteristics, it is important to keep track of what is going on with the other estimator. This can be done by looking at the cross-axis step response shown in figure 5.3 which shows how \hat{y} varies with a step input in x .

The cross-axis response is also independent of A . Unlike the cross-axis step response given by figure 4.4 which showed an unbounded increase in the cross-axis step response by reducing the scanning radius. Since the response is independent of A the size of the step is no longer important. The error is not only bounded but significantly smaller than the cross-axis step response of the traditional conical scanning estimator. The asymmetrical tracking which causes the track to curve to the origin is eliminated.

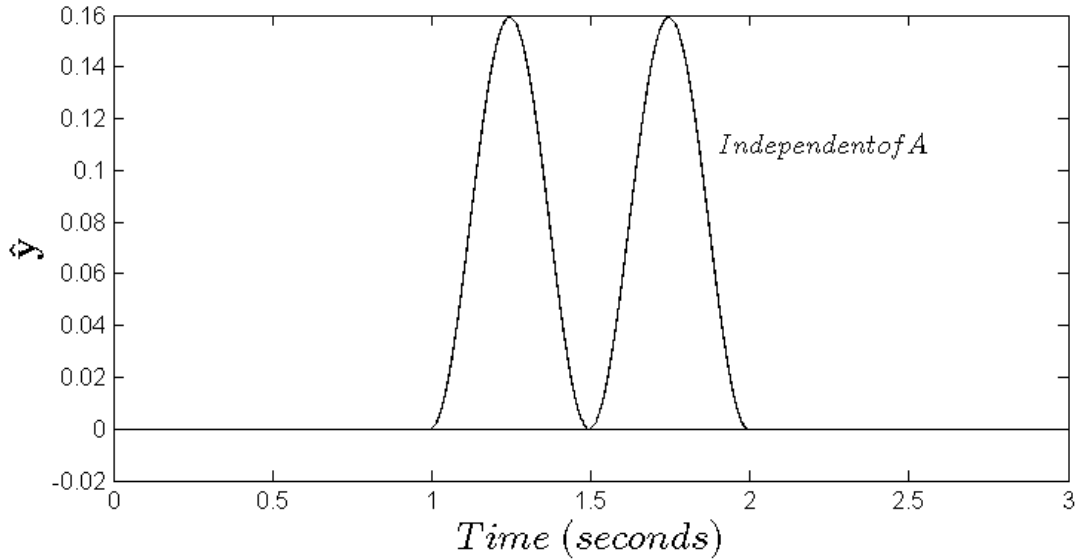


Figure 5.3: Cross-axis step response of the gradient conical scanning estimator with $\omega = 2\pi$ and $\phi = \frac{3\pi}{2}$ while varying A .

5.3 Ramp Response

While the step response is independent of A for the gradient conical scanning estimator, this is not the case for the ramp response. Figure 5.3 shows the ramp response for the gradient conical scanning estimator, and while it is independent of A , the error is bounded. It is apparent that the estimator averages slightly below the ramp response input line. This occurs due to the inherent time delay introduced in the system due to the integration over a full scan. This lag appears in the ramp response of the traditional conical scanning estimator as well but it is less apparent due to the significantly larger error accumulation.

While the estimator is no longer independent of A , it still has two advantages over the traditional estimator. First, the error is now bounded for a given A . The error does not accumulate unboundedly as more cycles are made, but rather oscillates between the maximum and minimum values chosen by the perturbing radius. Additionally, the error in estimate is much smaller than the error for the same value of A with the traditional conical scanning estimator.

The cross-axis ramp response has similar advantages over the response of the traditional conical scanning estimator. Just like the ramp response shown in figure 5.3, the cross-axis response in figure 5.3 depends on the perturbation radius A . However, just as

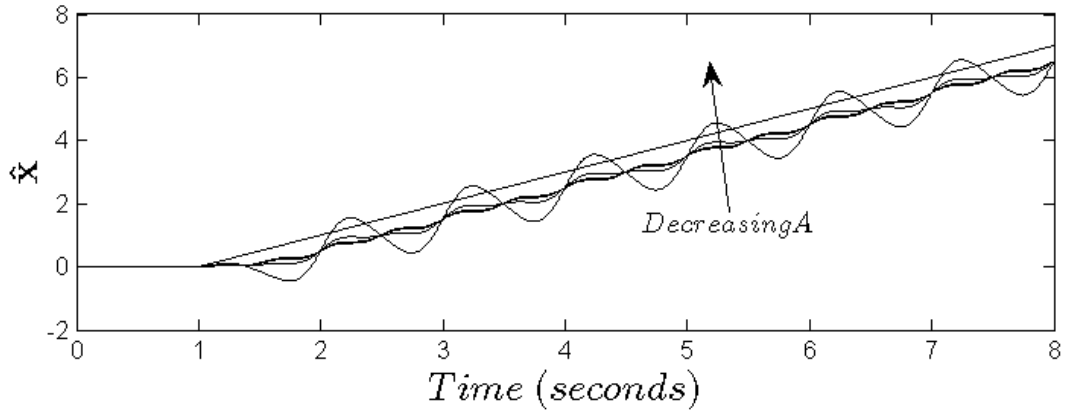


Figure 5.4: Ramp response of the gradient conical scanning estimator with $\omega = 2\pi$ and $\phi = \frac{3\pi}{2}$ while varying A .

in the ramp response the error is bounded, and does not increase over the course of the ramp. It is also significantly less sensitive to the amplitude A than the traditional conical scanning method.

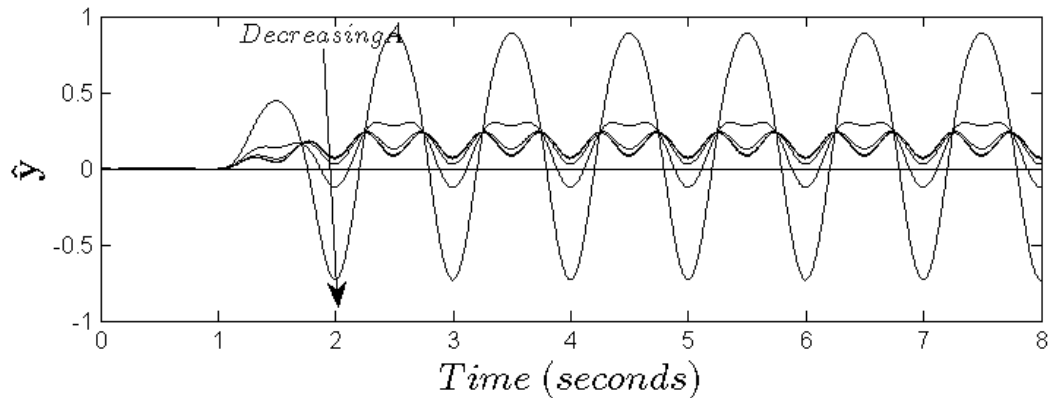


Figure 5.5: Cross-axis ramp response of the gradient conical scanning estimator with $\omega = 2\pi$ and $\phi = \frac{3\pi}{2}$ while varying A .

5.4 Noise Response

The noise response of the gradient conical scanning estimator is not as good as that of the traditional conical scanning estimator due to the added derivative term. The received signal strength is a noisy signal, and taking the derivative of such a signal just increases

the noise. The noise response of the estimator is significantly worse as most of the high frequency noise gets through.

Even though the noise response of the estimator is significantly worse, this may not have a dramatic effect on the closed loop system. The closed loop system acts as a low pass filter for the noise, and most of the higher frequency noise that makes it through the estimator will be at frequencies above the bandwidth of the control loop so the system will be unable to track them. This will effectively limit the effect of the noise and prevent the system from going unstable by not tracking the noise. The comparison of the closed loop system is done in chapter 6.

5.5 Problems

While the gradient estimator seems to be a significant improvement over the traditional estimator the largest problem comes from noise in the received signal strength. The noise response is the only performance metric which the gradient estimator does not do as well as the traditional conical scanning estimator. The noise ends up not being a large problem due to the low pass filtering capability of introducing the estimator to the closed loop system.

6: Closed Loop Simulation

In addition to analyzing the estimators individually, a simulation was performed of the closed loop system where the estimator was added back in and the output is fed through a PI feedback control back into the system dynamics. Figure 6.1 depicts the full closed loop traditional conical scanning system, including the tracking feedback.

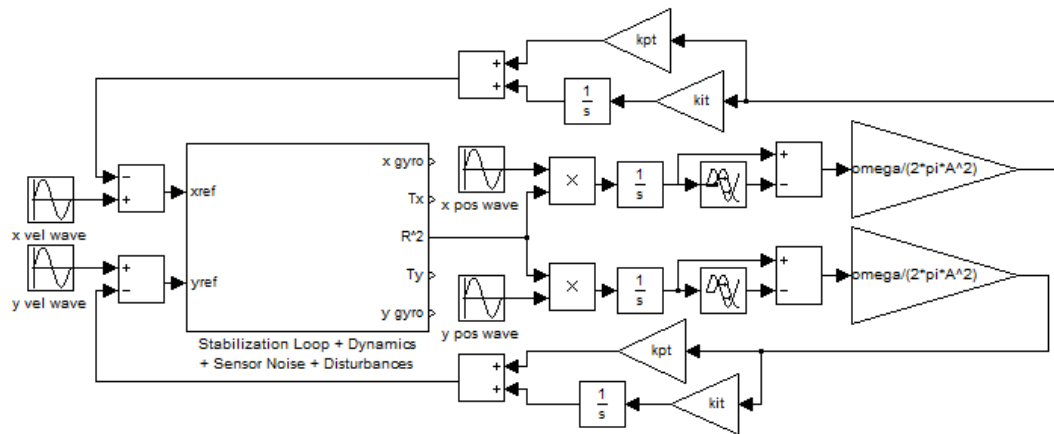


Figure 6.1: Closed loop system of the traditional conical scanning estimator including tracking feedback.

The closed loop system for the gradient conical scanning estimator is similar and is shown before in figure 6.1.

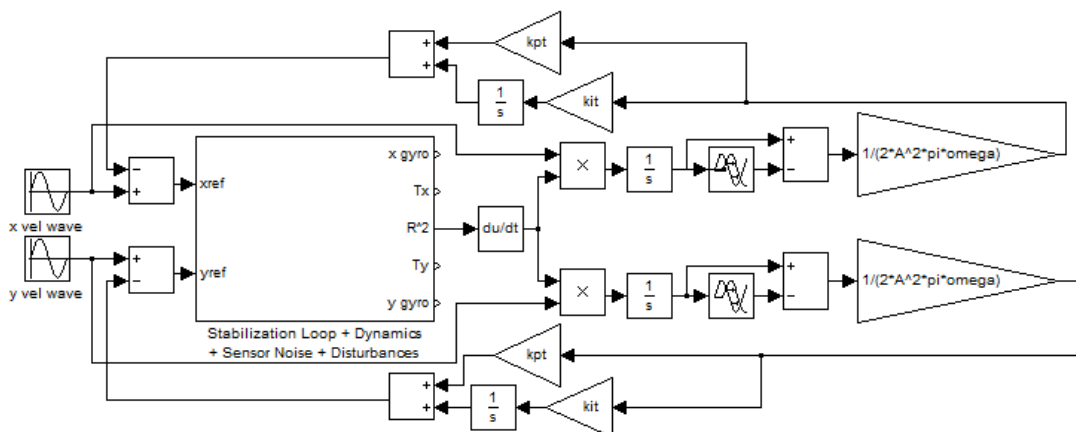


Figure 6.2: Closed loop system of the gradient conical scanning estimator including tracking feedback.

When running the simulation, varying values were used for kp_t and ki_t until the system went unstable. The gains were chosen by modeling the system as a mass spring system, and determining the parameters needed for critical damping. This showed that $ki_t = \frac{kp_t^2}{2}$ in order to get a reasonable phase margin for a given value for kp_t .

Using the traditional estimator with $A = 0.1$, and $\omega = 2\pi$, I was able to push kp_t up to 2.490 when starting from the (x, y) location $(0.1, 0)$ before the system went unstable.

Using the gradient estimator with $A = 0.1$, and $\omega = 2\pi$, I was able to push kp_t up to 2.605 when starting from the (x, y) location $(0.1, 0)$ before the system went unstable.

This increases the effective bandwidth of the system, allows for better tracking performance. The increase in bandwidth boosts performance, and allows for faster tracking.

7: Conclusions and Future Direction

7.1 Conclusions

Three new methods for peak seeking controllers were developed to solve the problem of pointing a receive only antenna at a remote satellite. All three of these estimators worked well in simulation, with the measured gradient conical tracking method being the largest breakthrough in control. However, the research focused on the gradient conical scanning estimator which modified the traditional conical scanning estimator by convolving the derivative of each signal rather than the signals themselves.

By performing a detailed analysis of the steady state and transient responses the following metrics were used to determine how good the estimator was.

- Steady State Response: Estimate produced after a full cycle while the system is in steady state conditions should match the real position exactly.
- Step Response: The step response in x from a unit input in the satellites position along x should remain near the range of $[0, 1]$.
- Ramp Response: The ramp response of the x estimator due to motion along the x axis should stay bounded around the position of the satellite over time.
- Cross-Axis Step Response: The step response in x from a unit input in the satellites position along y should remain near the range of $[0, 1]$.
- Cross-Axis Ramp Response: The ramp response of the x estimator due to motion along the y axis should stay bounded around the position of the satellite over time.
- Noise Response: The estimator should reject enough noise which is propagating through the system as possible so the noise does not cause the system to go unstable.

The new gradient conical scanning estimator outperforms the traditional conical scanning estimator against all metrics with the exception of the noise response. However, the extra noise introduced within the system does not cause the system to become unstable, but

rather is canceled out by the properties of the closed loop system. The closed loop system is able to have higher bandwidth with the gradient estimator which allows for better tracking performance.

The gradient conical scanning estimator is shown to be a theoretical improvement over the traditional estimator, and in cases without excessive amounts of noise, should outperform the traditional estimator. The gradient conical scanning estimator is the recommended estimator to us on mobile satellite communications antenna.

7.2 Future Work

The research presented is a thorough investigation of particular estimators, however, this research has produced quite a few new paths for future research.

7.2.1 Signal Saturation

Some of the instability in the system is generated by commanding forces which are too large for the system to handle. These large forces cause the antenna to move rapidly (due to the proportional feedback control) which causes the tracking loop to become unstable. By adding saturation limits to the feedback, or to the received signal strength it may be possible to increase the region of attraction around the origin and have a system which is stable from any initial position.

7.2.2 Parameter Optimization

Future work could be done to find the optimal parameters for a given system. By exploring the expected noise characteristics, it may be possible to optimize for the best scanning frequency, perturbation amplitude, or even estimator. This type of analysis should be carried out to determine how robust a particular method is to noise.

7.2.3 Measured Gradient Scanning and Tracking Systems

The effects of using the gyroscope measurements rather than the predicted velocities were not explored through the course of this project. A more in-depth analysis of the effect

from using gyroscope measurements could be made to better predict the characteristics of this model. In addition to using the measurements, the effect the internal noise has on observability is another topic which could be explored. I showed through simulation that noise has enough observability to track to the origin, but bounds on noise have not been provided.

7.2.4 Hardware Implementation

While the theoretical grounding for the new estimators shows they will work better in certain conditions than the traditional conical scanning estimator, it is important that a hardware test under real world conditions is performed to determine if the assumptions made in the thesis can be validated. Work is ongoing to implement the gradient conical scanning estimator on a hardware platform.

Bibliography

- [1] D. F. Chichka, J. L. Speyer, C. Fanti, and C. G. Park. Peak-seeking control for drag reduction in formation flight. *Journal of Guidance Control and Dynamics*, 29(5):1221–1230, 2006.
- [2] J. Debruin. Control systems for mobile satcom antennas - establishing and maintaining high-bandwidth satellite links during vehicle motion. *IEEE Control Systems Magazine*, 28(1):86–101, 2008.
- [3] J.E. Ohlson, M.S. Reid, United States. National Aeronautics, and Space Administration. *Conical-scan tracking with the 64-m-diameter antenna at Goldstone*. JPL technical report. California Institute of Technology, Jet Propulsion Laboratory, 1976.
- [4] N. O. Perez-Arancibia, J. S. Gibson, T. C. Tsao, and IEEE. *Laser Beam Pointing and Stabilization by Intensity Feedback Control*, pages 2837–2842. Proceedings of the American Control Conference. IEEE, New York, 2009.